Citrobacter rodentium colitis evokes post-infectious hyperexcitability of mouse nociceptive colonic dorsal root ganglion neurons

Charles Ibeakanma, Marcela Miranda-Morales, Michele Richards, Francisco Bautista-Cruz, Nancy Martin, David Hurlbut and Stephen Vanner

Gastrointestinal Diseases Research Unit, Kingston General Hospital, Queen's University, Kingston, Ontario, Canada K7L 2V7

To investigate the possible contribution of peripheral sensory mechanisms to abdominal pain following infectious colitis, we examined whether the *Citrobacter rodentium* mouse model of human *E. coli* infection caused hyperexcitability of nociceptive colonic dorsal root ganglion (DRG) neurons and whether these changes persisted following recovery from infection. Mice were gavaged with *C. rodentium* or distilled water. Perforated patch clamp recordings were obtained from acutely dissociated Fast Blue labelled colonic DRG neurons and afferent nerve recordings were obtained from colonic afferents during ramp colonic distensions. Recordings were obtained on day 10 (acute infection) and day 30 (infection resolved). Following gavage, colonic weights, myeloperoxidase (MPO) activity, stool cultures, and histological scoring established that infection caused colitis at day 10 which resolved by day 30 in most tissues. Electrophysiological recordings at day 10 demonstrated hyperexcitability of colonic DRG neurons (40% mean decrease in rheobase, $P = 0.02$; 50% mean increase in action potential discharge at twice rheobase, $P = 0.02$). At day 30, the increase in action potential discharge persisted (∼150% increase *versus* control; $P = 0.04$). In voltage clamp studies, transient outward (I_A) and delayed rectifier (I_K) currents were suppressed at day 10 and I_A currents remained suppressed at day 30. Colonic afferent nerve recordings during colonic distension demonstrated enhanced firing at day 30 in infected animals. These studies demonstrate that acute infectious colitis evokes hyperexcitability of colonic DRG neurons which persists following resolution of the infection and that suppression of I_A currents may play a role. Together, these findings suggest that peripheral pain mechanisms could contribute to post-infectious symptoms in conditions such as post-infectious irritable bowel syndrome.

(Received 13 January 2009; accepted after revision 26 May 2009; first published online 26 May 2009)
Corresponding author S. Vanner: Kingston General Hospital, GIDRU Wing, 76 Stuart Street, Kingston, Ontario, Canada K7L 2V7. Email: vanners@hdh.kari.net

Abbreviations DRG, dorsal root ganglion; IBS, irritable bowel syndrome; MPO, myeloperoxidase; PI-IBS, post-infectious irritable bowel syndrome.

Visceral hyperalgesia, or exaggerated sensitivity to nociceptive stimuli, is often preceded by intestinal inflammation. For example, irritable bowel syndrome (IBS) (Thabane *et al.* 2007), a common disorder which exhibits visceral hyperalgesia, frequently occurs following an infectious gastroenteritis. Bacterial gastroenteritis is the strongest predictive factor identified to date for the development of IBS (Rodriguez & Ruigomez, 1999). Patients typically complain of abdominal pain and diarrhoea-predominant symptoms, and symptoms often persist for years (Spiller, 2007). Post-infectious IBS (PI-IBS) was first described more than five decades ago and was best characterized following the large outbreak in Walkerton, Canada, affecting 2700 residents through contaminated water supply with *Escherichia coli* 0157:H7, *Campylobacter jejuni*, and other pathogens (Marshall *et al.* 2006). In this study ∼30% of infected individuals developed PI-IBS and a recent meta-analysis among all available studies suggests the pooled incidence of PI-IBS is 10% (Thabane *et al.* 2007). Hence, PI-IBS is a common cause underlying IBS. A better understanding of the mechanisms involved could have an important impact on treatment and prevention of symptoms associated with this and related disorders.

There is considerable evidence from human studies that the abdominal pain experienced by PI-IBS patients results from dysregulation of sensory neural pathways (Kellow *et al.* 1991; Whitehead & Crowell, 1991). This

 DOI: 10.1113/jphysiol.2009.169110

abnormality could result from peripheral mechanisms (e.g. altered signalling in dorsal root ganglia neurons), central mechanisms (e.g. heightened perception of pain), or possibly both (Azpiroz *et al.* 2007). Peripheral mechanisms may be particularly important in PI-IBS given the observations that patients have altered mucosal permeability and there is evidence for persistent low levels of inflammation following resolution of the infection (Tornblom *et al.* 2002; Marshall *et al.* 2004) but study of peripheral mechanisms in humans is limited by the lack of accessibility. The findings from animal models of chemically induced colitis, which results in a severe transmural inflammatory process, demonstrate that during active inflammation colonic nociceptive dorsal root ganglion (DRG) neurons are hyperexcitable. Whether these changes are representative of those which would result from an acute bacterial infection of the colon where the severity and nature of the inflammation differs, however, is not clear. Moreover, to understand PI models such as IBS, it is particularly important to know whether changes in excitability persist after the infection and acute inflammation have resolved.

Human *E. coli* colitis can be modelled by the *Citrobacter rodentium* murine model of self-limiting colitis, providing an opportunity to examine the role of peripheral mechanisms in an animal model of bacterial infection. These bacteria attach and efface in a similar fashion to *E. coli* and cause a similar self-limiting inflammation (Barthold *et al.* 1978; Ghaem-Maghami *et al.* 2001; Wiles *et al.* 2006). Given the close resemblance of this infection to the human *E. coli* infection, a common cause of PI-IBS, we utilized this model to examine the possible role of bacterial infection in modulating peripheral sensory mechanisms following resolution of the infection and overt inflammation. We used retrograde labelling to enable nociceptive DRG neurons innervating the infected region of the colon to be examined using patch clamp and afferent nerve recording techniques to address two central aims. Firstly, the excitability of the colonic neurons was examined during the acute infection to determine if inflammation induced by bacteria causes neuronal hyperexcitability, as seen with more severe chemically induced inflammations. Secondly, neurons were studied at day 30, a time point at which previous studies have shown that infection and inflammation have resolved (Khan *et al.* 2006; Skinn *et al.* 2006), to determine if changes in excitability of the neurons persisted, and if so, what ionic mechanism may be involved.

Methods

C. *rodentium* model of colitis

C57BL/6 mice (20–25 g) of either sex were obtained from Charles River Laboratories (Montreal, QC, Canada). All protocols were approved and monitored by the Queen's University Animal Care Committee and conformed to the Guidelines of the Canadian Council of Animal Care. The authors have read the journal policy and UK regulations on animal experimentation (Drummond, 2009) and their experiments comply with the policies and regulations. Mice were killed by cervical transaction following induction of general anaesthesia using isoflurane (Baxter Corporation; Mississauga, ON, Canada) inhalation.

Mice were gavaged with 6.6×10^{11} colony forming units of *C. rodentium* (strain DBS 100) as previously described (Luperchio & Schauer, 2001; Mundy *et al.* 2005) or with distilled water. Daily subcutaneous injections of 0.5 ml lactated Ringer solution were given for a week to avoid dehydration, and mice were monitored for feeding, signs of pain, and weight loss throughout the experimental period. Mice were studied at day 10 (active infection) and day 30 (after resolution of infection).

At day 3 or day 20 after *C. rodentium* or distilled water were gavaged, surgeries were performed on mice to label colonic DRG neurons with Fast Blue fluorescent retrograde label (Cedarlane Laboratories; Homby, ON, Canada), as previously described (Beyak *et al.* 2004; Kayssi *et al.* 2007). The different time points were chosen to ensure Fast Blue labelling was not lost by day 30. Briefly, mice were anaesthetized with intra-peritoneal injection (0.1 ml/10 g body wt) of a combination of ketamine (Pfizer; New York) (18.75 mg ml^{-1}) and xylazine (Bayer; Etobicoke, ON, Canada) (1.25 mg ml^{-1}). A midline laparotomy was then performed to expose the descending colon. Under a dissecting microscope, 17 mg ml^{-1} Fast Blue was injected (10 μl per injection) into 5–10 sites along the colon wall. The colon was replaced and the wound sutured with 4.0 silk. Buprenex (Buprenorphine 0.25 μ g (g body wt)$^{-1}$ I.P.) was given to control post-operative pain. Animals were allowed to recover on a warm blanket, monitored for signs of pain and given free access to food and water.

Cell preparation

At day 10 or day 30 following *C. rodentium* gavage, DRG neurons were acutely dissociated from T_9 to T_{13} ganglia or from T_1 to T_3 (for studies with non labelled neurons from a region of the spinal cord which does not innervate the colon), as previously described (Moore *et al.* 2002; Stewart *et al.* 2003). Briefly, tissue was incubated in collagenase (Worthington; Lakewood, NJ, USA) (1 mg ml^{-1}) and dispase (Roche; Indianapolis, IN, USA) (4 mg ml^{-1}) for 15 min at 37°C, triturated with a fire-polished Pasteur pipette. Dispersed neurons were suspended in DMEM (pH 7.2–7.3) containing 10% fetal bovine serum, 100 U ml^{-1} Penicillin, 0.1 mg ml^{-1} Streptomycin, and

2 mM glutamine, plated on PureCol-coated (60 μl ml^{-1}) (Inamed Biomaterials, Fremont, CA, USA) cover slips and incubated overnight in a humidified incubator at 95% O_2 and 5% CO_2 until retrieval for electrophysiological studies.

Electrophysiological recordings

Perforated patch clamp experiments were performed in current or voltage clamp modes at room temperature. Fast Blue labelled neurons were identified by their bright blue fluorescence under brief exposure to ultraviolet light, using a U-MWIG2 filter. Only small neurons ($\leq$40 pF capacitance; i.e. large Fast blue labelled neurons were not studied) were studied because these neurons have been shown to display properties associated with nociceptors (i.e. capsaicin sensitivity, TTX-resistant action potentials) (Akopian *et al.* 1996; Rush *et al.* 1998; Cummins *et al.* 1999; Yoshimura & de Groat, 1999; Moore *et al.* 2002; Beyak & Vanner, 2005). Signals were acquired using an Axopatch 200B amplifier and digitized with a Digidata 1322A A/D converter (Axon Instruments/Molecular Devives, Sunnyvale, CA, USA). Signals were low-pass filtered at 5 kHz, acquired at 20 kHz, stored and analysed using Clampfit 10.0 (Axon Instruments). Capacitive transients were corrected using analogy circuitry. Inclusion criteria for analysis of cells in current clamp mode were resting membrane potentials more negative than −40 mV and overshooting action potentials with a hump on the falling phase.

Perforated patch recordings were obtained using Amphotericin B (240 μg ml^{-1}) from Sigma (St Louis, MO, USA) as described previously (Cooper *et al.* 1990; Rae *et al.* 1991). Due to the compound's photosensitivity and rapid rate of breakdown upon exposure to light, mixed Amphotericin B solutions were replaced every 2–3 h. Solutions (in mM) were as follows; extracellular solution: 140 NaCl, 5 KCl, 1 $MgCl_2$, 2 $CaCl_2$, 10 Hepes, 10 D-glucose, pH 7.4; pipette solution: 110 potassium gluconate, 30 KCl, 10 Hepes, 1 $MgCl_2$, 2 $CaCl_2$, pH 7.25. The liquid junction potential was taken to be 12 mV, and corrected for. For isolation of potassium currents in voltage clamp recordings the following solutions were used; extracellular: 140 NMDG, 4 KCl, 1.8 Hepes, 1 D-glucose, 1 $CaCl_2$, 1 $MgCl_2$, pH 7.4; pipette solution: 110 potassium aspartate, 30 KCl, 10 EGTA, 10 Hepes, 2 Na_2-ATP, 1 $MgCl_2$, pH 7.2. The liquid junction potential was calculated to be 7.3 mV and corrected for. I_A and I_K currents were separated based on their biophysical properties, as previously described (Stewart *et al.* 2003). Briefly, total K^+ current was elicited from a holding potential of −100 mV with depolarizing pulses in 10 mV increments between −90 mV and +50 mV. These steps were repeated with I_A inactivated by using a holding potential of −60 mV, and the traces subtracted to provide I_A. I_A inactivation properties were studied using a two pulse protocol as previously described (Stewart *et al.* 2003): a 1 s pre-pulse varying between −120 and 0 mV, followed by a 400 ms test pulse of +50 mV. Currents during the test pulse were normalized and plotted against the conditioning potential and fitted with the Boltzmann function:

$$I/I_{\max} = I/(I + \exp[V_{50} - V_m/k]),$$

where I is the current, $I_{\max}$ is the maximal current, V_{50} is the membrane potential for half-activation, V_m is the command potential, and k is the slope factor.

Recording of afferent nerve activity in response to intraluminal distension pressure

Experiments were performed on *C. rodentium* infected or sham animals at day 10 or 30. Animals were killed by cervical dislocation and their abdominal cavity opened. The distal colon and rectum were dissected from the pelvis with attached mesenteric nerves and placed in a Sylgard-lined organ chamber which was continually perfused with oxygenated Krebs solution (in mM: 118.4 NaCl, 24.9 $NaHCO_3$, 1.9 $CaCl_2$, 1.2 $MgSO_4.7H_2O$, 1.2 KH_2PO_4, 11.7 D-glucose) at a flow rate of ∼8 ml min^{-1} and maintained at 33–34°C. Proximal and distal ends of the bowel were securely attached to an input and outlet port. The input port was connected to a perfusion syringe pump, which allowed continuous intraluminal perfusion of Krebs solution through the segments (0.2 ml min^{-1}) or periodic distension when closed. Intra-luminal pressure was recorded via a pressure amplifier (NL 108, Digitimer, UK) connected in parallel with the input port. The mesenteric bundle was pinned out to the base of the chamber and a mesenteric nerve was dissected out from the bundle and drawn into a suction electrode. The electrical activity was recorded by a Neurolog headstage (NL 100, Digitimer Ltd, UK), amplified (NL104), and filtered (NL125 band pass 200–3000 Hz) and acquired (20 kHz sampling rate) to a PC through a Micro 1401 MKII interface running Spike 2 software (Cambridge Electronic Design (CED), Cambridge, UK). The preparation was stabilized for 30 min and was distended to an intra-luminal pressure of 60 mmHg with closure of the outlet port. Only afferent discharge responses to ramp distensions that were stable and reproducible (at least 3 times 10 min apart) were analysed. The third response was analysed in each case.

Evaluation of colonic inflammation

Histopathology assessment. At day 10 or day 30 post-infection with *C. rodentium* or control distilled water, colon samples were taken for pathological assessment.

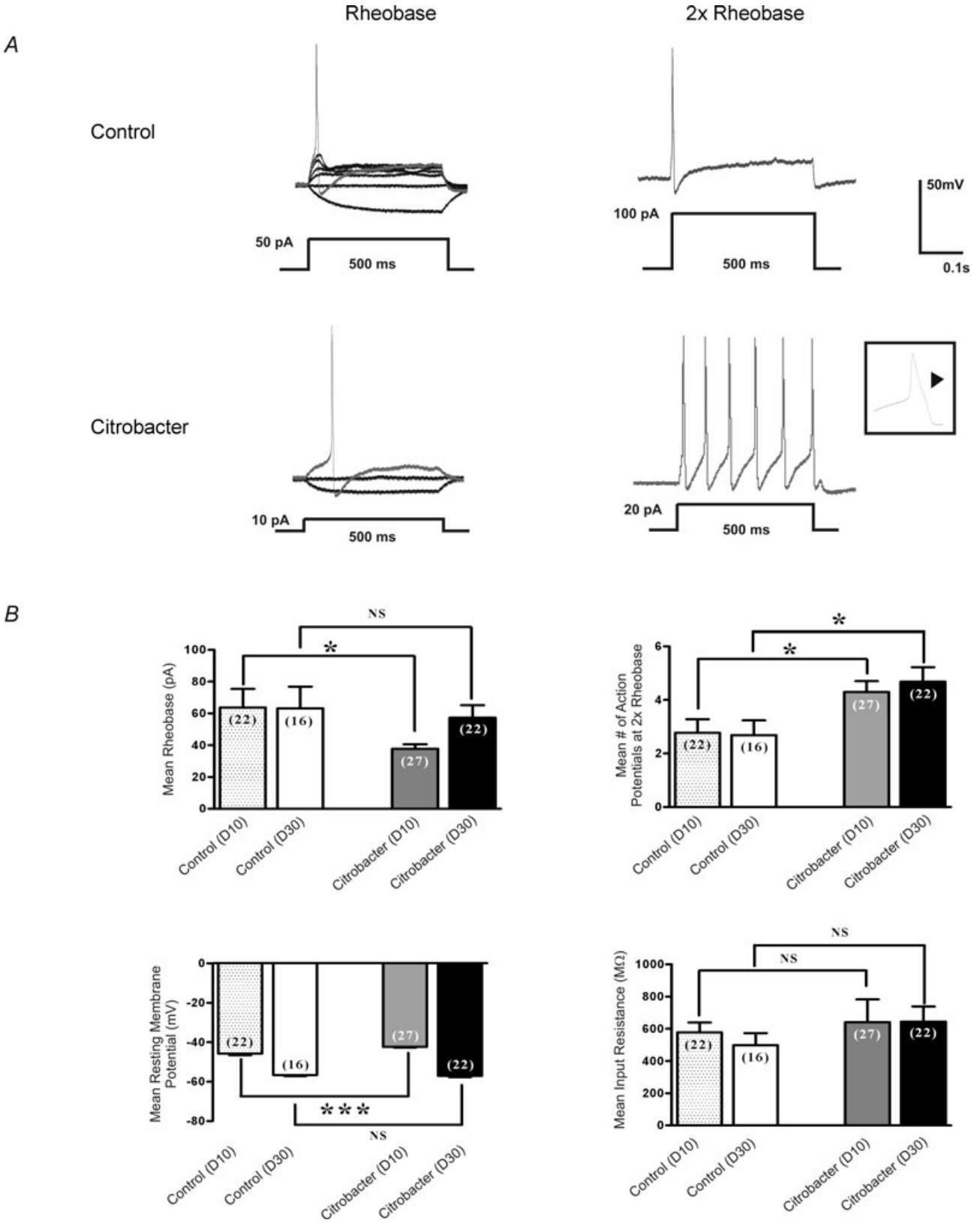

Full thickness colonic tissue samples for histological assessment were fixed in 10% neutral buffered formalin. Following paraffin embedding, 5 μm thick sections (3 cross sections from each colon specimen/block) were cut and stained with hematoxylin and eosin (H&E). Slides were reviewed by a pathologist (D.H.) who was blinded to study group origin. *C. rodentium* or sham treated colonic tissues were also stained with Toluidine Blue to identify mast cells (Tuna *et al.* 2006).

Assessment of colonic pathology utilized a semi-quantitative colitis histological scoring system that evaluated and scored for inflammation and crypt height. Inflammation score (score range 0–9) was determined by assessment of (a) presence and intensity of mononuclear cell infiltrate (0, none; 1, mild; 2, moderate; 3, severe), (b) presence and intensity of neutrophilic cell infiltrate (0, none; 1, mild; 2, moderate; 3, severe), (c) maximum depth of mural inflammatory infiltrate (0, none; 1, mucosa; 2, mural), and (d) mucosal lymphoid hypertrophy (0, absent; 1, present). Mean crypt height (in micrometres) was calculated for each specimen from individual measurements (at least 5; most cases greater than 15) of the lengths of all well oriented crypts on each specimen slide using an ocular micrometer.

Myeloperoxidase (MPO) enzyme assay. Briefly, full thickness distal colon tissues from *C. rodentium* and control gavaged mice were collected and assayed for enzyme activity, as previously described (Bradley *et al.* 1982).

Statistical analysis

Results were tested with unpaired Student's *t*-test or 2-way ANOVA with Bonferroni's *post hoc* test and the significance was set at $P < 0.05$. Data are expressed as means ± S.E.M. Fitting of data was done using the Boltzmann equation fit function in Origin 6.0 (OriginLab Corp., Northampton, MA, USA). Voltages of half-activation (V_{50}) and slope factors (k) were obtained from the individual Boltzmann curve fits. The mean firing frequency (impulses (imp) s^{-1}) were measured with a time constant of 10 s. Firing rates were measured using a bin width of 1 s while the stimulus–response curves for whole nerve activity were constructed for 5 mmHg increments using customized script program (CED).

Results

Effects of *C. rodentium* induced colitis at day 10 on neuronal excitability

All animals were monitored daily and most infected animals (85–90%) exhibited signs of a brief illness for 2–3 days following gavage (e.g. decreased activity) but recovered quickly. A small number of animals were sicker for a more extended period but by 7–10 days there were no observable differences from the controls. There was a 2–3% mortality rate which occurred within the first 3 days following infection.

The excitability of Fast Blue labelled DRG neurons was determined by measuring differences in membrane potential, rheobase, number of action potentials at twice rheobase, and input resistance (Fig. 1), as previously described (Beyak *et al.* 2004; Malykhina *et al.* 2006; Moore *et al.* 2002). Individual cells in all current clamp experiments were obtained from $\geq$ 5 animals (total number = 33 animals) in each series of experiments. In current clamp mode, recordings were obtained from small Fast Blue labelled DRG neurons from animals infected with *C. rodentium* ($n = 27$ cells), and controls ($n = 22$ cells) (Fig. 1*A* and *B*). At day 10 (Fig. 1*B*), where infection and inflammation were established, the mean rheobase was significantly decreased (mean = 37.8 *vs.* 63.6 pA;

Figure 1. Effects of *C. rodentium* induced colitis on excitability of colonic DRG neurons
A, representative current clamp trace of action potential elicited at rheobase and two times rheobase from labelled neurons isolated from *C. rodentium* treated and control animals. The amount of current needed to elicit an action potential is significantly lower in labelled *C. rodentium* neurons (10 pA) compared to control neurons (50 pA). Furthermore, the *C. rodentium* neurons fire significantly more action potentials at 2× rheobase compared to control neurons. Action potential tracings from control neurons are shown in upper panel and those from *C. rodentium* treated neurons are shown in lower panel. A 500 ms depolarising current pulse was used to elicit the action potentials. Inset shows one of the action potentials using expanded time scale to exhibit the characteristic hump on the falling phase typical of nociceptive neurons. *B*, data summarizing changes in electrophysiological properties of nociceptive DRG neurons during acute infection (day 10) and following resolution of infection (day 30). *C. rodentium* induced colitis caused a significant reduction in rheobase, significant increase in the mean number of action potentials at 2× rheobase and a significant reduction in the mean resting membrane potential in labelled neurons isolated from *C. rodentium* treated (grey filled bars) animals during acute infection compared to matched controls (stippled bars). The mean input resistance did not change significantly. Data are means ± S.E.M. $^*P < 0.05$; NS, not significant. At day 30, neurons from *C. rodentium* treated (black filled bars) animals fired significantly more action potentials at 2× rheobase compared to controls (open bars) whereas, the mean rheobase, resting membrane potential and input resistance returned to comparable control values. Data are means ± S.E.M. $^*P < 0.05$.

Table 1. *C. rodentium* enumeration in faecal samples

	Day 10	Day 15	Day 20	Day 25	Day 30
Control (CFU (g pellet)$^{-1}$)	0.00 ± 0.00 ($n = 9$)	0.00 ± 0.00 ($n = 4$)	0.00 ± 0.00 ($n = 4$)	0.00 ± 0.00 ($n = 4$)	0.00 ± 0.0 ($n = 8$)
Citrobacter (CFU (g pellet)$^{-1}$)	$5.0 \times 10^5 \pm 461661$ ($n = 10$)	0.00 ± 0.00 ($n = 4$)	0.00 ± 0.00 ($n = 4$)	0.00 ± 0.00 ($n = 4$)	0.00 ± 0.0 ($n = 14$)

$P = 0.02$), compared to controls. The mean number of action potentials at twice rheobase was also significantly increased in the *C. rodentium* group compared to controls (4.3 *vs.* 2.8 respectively; $P = 0.02$). The mean resting membrane potential was slightly lower in the *C. rodentium* group compared to controls (mean -54.4 ± 0.4 mV *vs.* -57.9 ± 0.7 mV; $P = 0.0001$). In contrast, the mean input resistance did not differ between the two groups.

The excitability of DRG neurons which did not innervate the inflamed colon (from ganglia in T1-T3 at day 10 in *C. rodentium* infected mice and controls) was also compared. No difference in the rheobase or number of action potentials at twice the rheobase was observed between the infected ($n = 11$ cells) and non-infected animals ($n = 15$ cells) (rheobase $= 66.4 \pm 9.2$ pA for *C. rodentium* infected and 69.3 ± 8.1 pA for control cells, respectively; number of action potentials at twice rheobase $= 2.3 \pm 0.6$ for *C. rodentium* infected and 2.1 ± 0.4 for controls).

Neuronal hyperexcitability persists after resolution of acute infection

Previous studies suggest that infection and inflammation resolve by day 30 following oral inoculation with *C. rodentium* (Khan *et al.* 2006; Skinn *et al.* 2006). Hence, we used the day 30 time point to examine whether changes in neuronal excitability were still evident following resolution of the infection. At this time point, we found that the mean number of action potentials at twice rheobase was still markedly increased (mean $= 4.1$, $n = 22$ cells *vs.* 2.5, $n = 16$ cells; $P < 0.04$) compared to controls (Fig. 1*B*). These changes were similar to those observed at day 10, suggesting these changes were sustained following their induction with the initial infection. In contrast, other parameters of excitability (rheobase and resting membrane potential) returned to values similar to that observed for controls (Fig. 1*B*).

Monitoring of *C. rodentium* infection and colitis

Four parameters of infection and inflammation were monitored in samples obtained from animals used in the electrophysiological experiments. Fecal samples, colon weight, MPO activity and histological scores were studied to confirm the evolution of infection and inflammation. Faecal pellets were cultured for bacteria at days 10, 15, 20, and 30 (Table 1). *C. rodentium* organisms were absent by day 15.

During active infection (day 10), the mean wet weight per length of colon from the *C. rodentium* group ($n = 13$ colons) was almost 70% greater compared to uninfected controls ($n = 9$ colons; $P < 0.0002$). Following resolution of infection (day 30), this had returned to comparable control levels ($n = 14$ colons for *C. rodentium* and 12 colons for control groups) (Fig. 2*A*). Similarly, MPO activity was markedly increased in colonic tissues at day 10 ($n = 5$ colonic tissues for *C. rodentium* and 6 colonic tissues for control groups) and values had returned to control levels when measured at day 30 ($n = 7$ colonic tissues for *C. rodentium* and 6 colonic tissues for control groups) (Fig. 2*B*).

Although previous studies have suggested that inflammation induced by *C. rodentium* had resolved by day 30 (Khan *et al.* 2006; Skinn *et al.* 2006) and this was also suggested by our MPO data and wet weight measurements (Fig. 2), we also conducted a careful histological assessment by a GI pathologist, who was blinded to the presence or absence of infection, to provide a sensitive measure of subtle inflammation at this time point (Fig. 3*A* and *B*). Microscopic damage scores demonstrated a marked increase in the inflammation composite score (range 3–6; $P < 0.0001$) and crypt hyperplasia at day 10 in colons infected with *C. rodentium* compared to controls (Fig. 3*A* and *B*). At day 30, most tissues could not be distinguished from controls, but our detailed histological scoring system suggested there was a mild residual inflammation in some animals (control range 0–2, *C. rodentium* 0–3; see Fig. 3*B*). Unlike the tissues from infected animals at day 10 where neutrophils were prominent, tissues from day 30 animals rarely exhibited neutrophils in keeping with the MPO measurements. Although subtle inflammation can be a feature of IBS (Marshall *et al.* 2004; Tornblom *et al.* 2002), we conducted a *post hoc* evaluation of neurons from tissues whose histological scores were in the same range as controls (i.e. histological scores 0) to eliminate any possible contribution this low level inflammation might have in the measured level of excitability. Control recordings were obtained from animals in the same batch (i.e. each animal in a batch of 6 had a matched control to minimize for biological variability between batches of animals). This *post hoc* analysis of neurons from 'non-inflamed' tissue also showed the 2- to 3-fold increase

in numbers of action potentials at twice the rheobase (Fig. 3*C*), demonstrating that neurons innervating tissues considered to be non-inflamed by a GI pathologist, remained hyperexcitable.

We also examined mast cell numbers at day 10 and day 30 using Toluidine Blue. We found small numbers of mast cells at day 10, largely in the extra-mucosal bowel wall (Fig. 4; $n = 5$ colons at each time point) and only a rare mast cell was evident at day 30. Only a very small numbers of mucosal mononuclear cells were observed at day 30 and these did not differ from controls.

Suppression of K_V currents contributes to sustained hyperexcitability at day 10 and 30

The finding at day 10 and 30 of a sustained increase in number of action potentials at twice the rheobase could suggest that I_A currents were suppressed given their prominent role in regulating action potential discharge (Connor & Stevens, 1971; Tierney & Harris-Warrick, 1992; Amberg *et al.* 2002). Previous studies of acute visceral inflammation have shown that suppression of I_A currents is a common mechanism underlying DRG neuronal hyperexcitability during active inflammation but it is unknown whether these changes might persist in non-inflamed tissues (Stewart *et al.* 2003; Tan *et al.* 2006). Therefore, we employed voltage clamp electrophysiological methods to determine whether modulation of these currents could play a role in the sustained excitability at days 10 and 30. Individual cells were obtained from ≥ 5 animals (total number = 28) for each series of voltage clamp experiments. Using voltage clamp protocols, as previously described (Beyak & Vanner, 2005; Stewart *et al.* 2003), I_A and I_K currents were separated

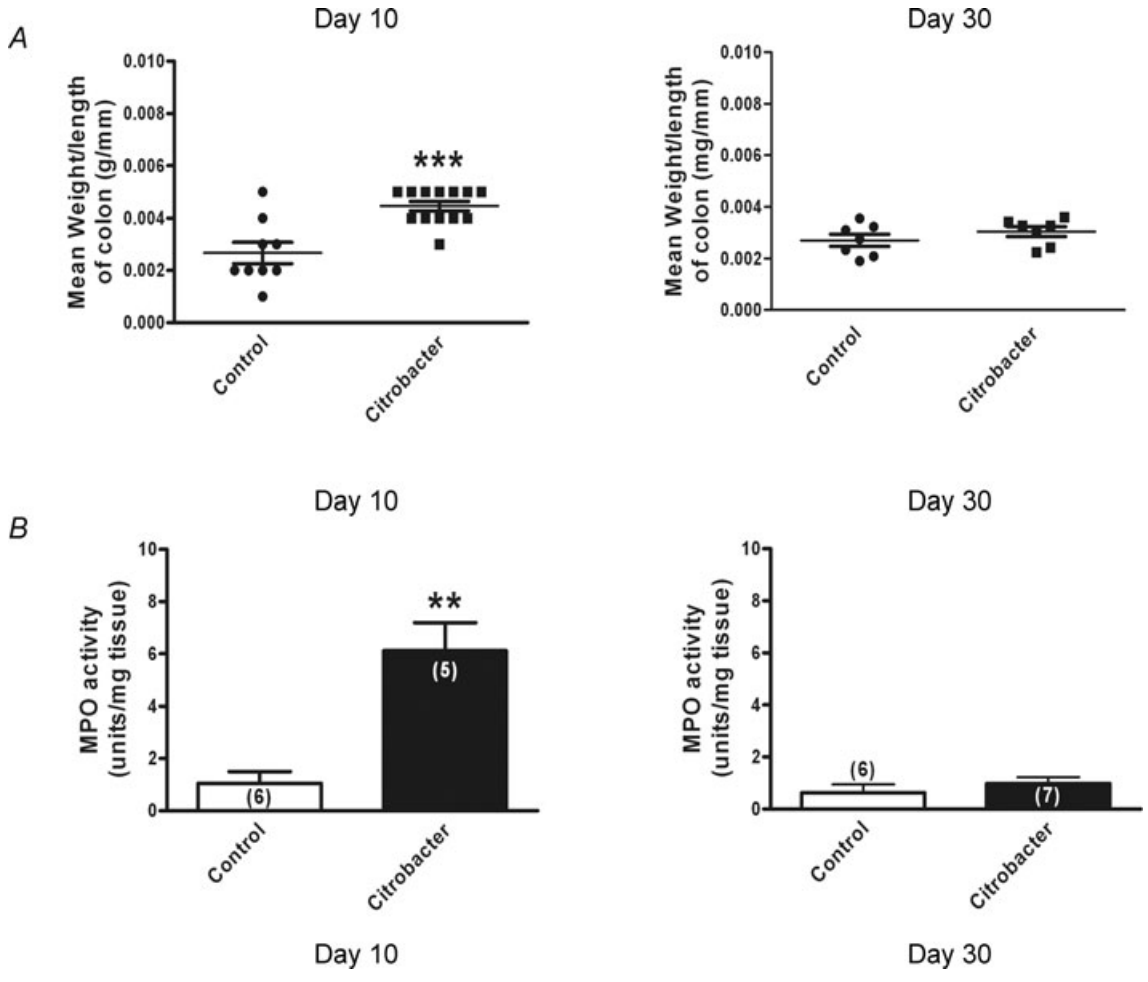

Figure 2. Monitoring of *C. rodentium* colitis
A, scatter plot of colonic wet weight during active infection (day 10) ($n = 13$ animals for *C. rodentium* and 9 animals for control); $^{***}P < 0.0002$ and following resolution (day 30) of infection ($n = 7$ animals for both *C. rodentium* and control). The lines show the mean ± S.E.M. for each treatment group. *B*, increased MPO activity was detected during acute infection (day 10) in tissue samples from *C. rodentium* infected animals (filled bars) compared to controls (open bars), whereas levels were comparable to control values on resolution of the infection (day 30). Data are mean ± S.E.M. values; $^{**}P < 0.005$.

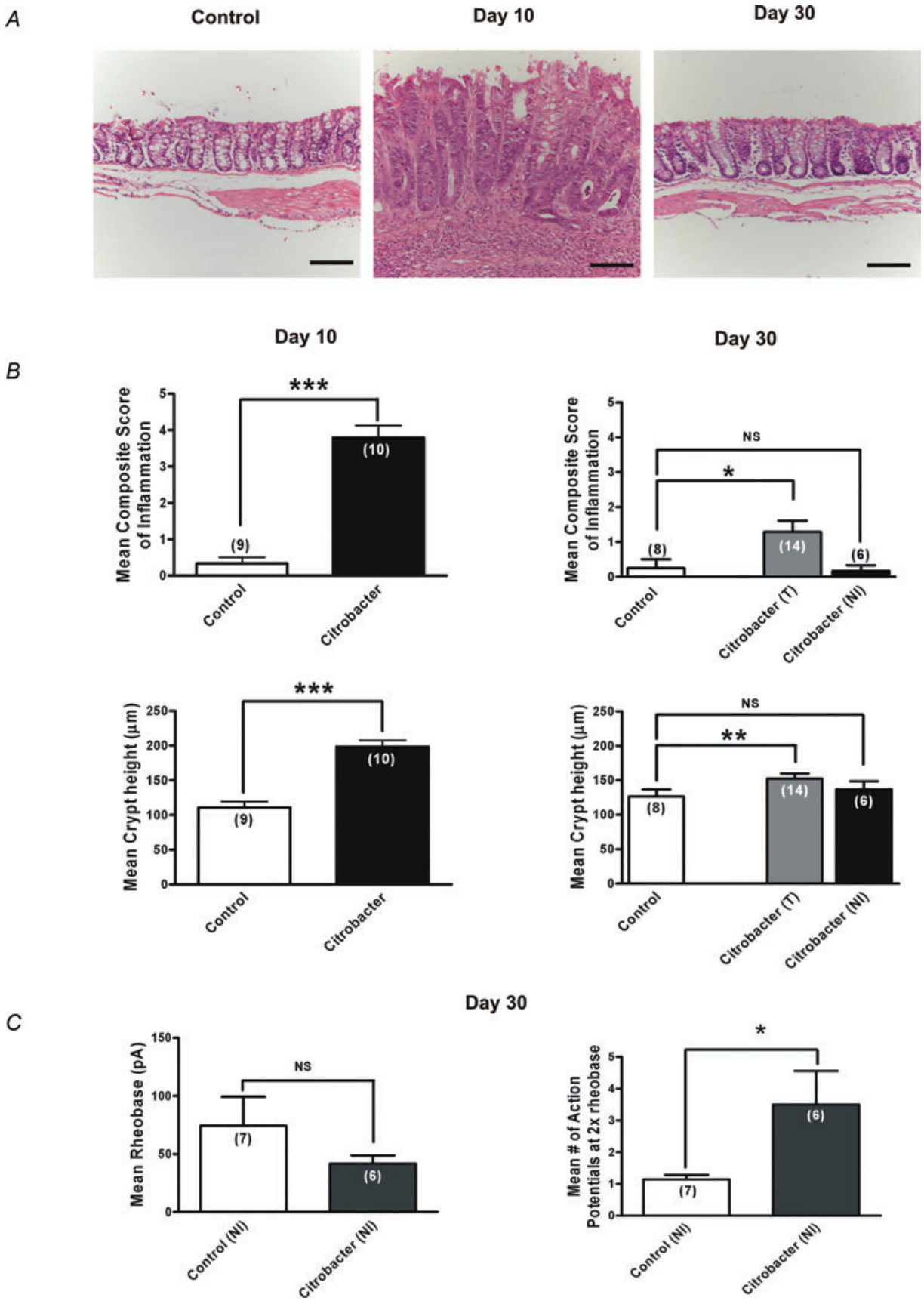

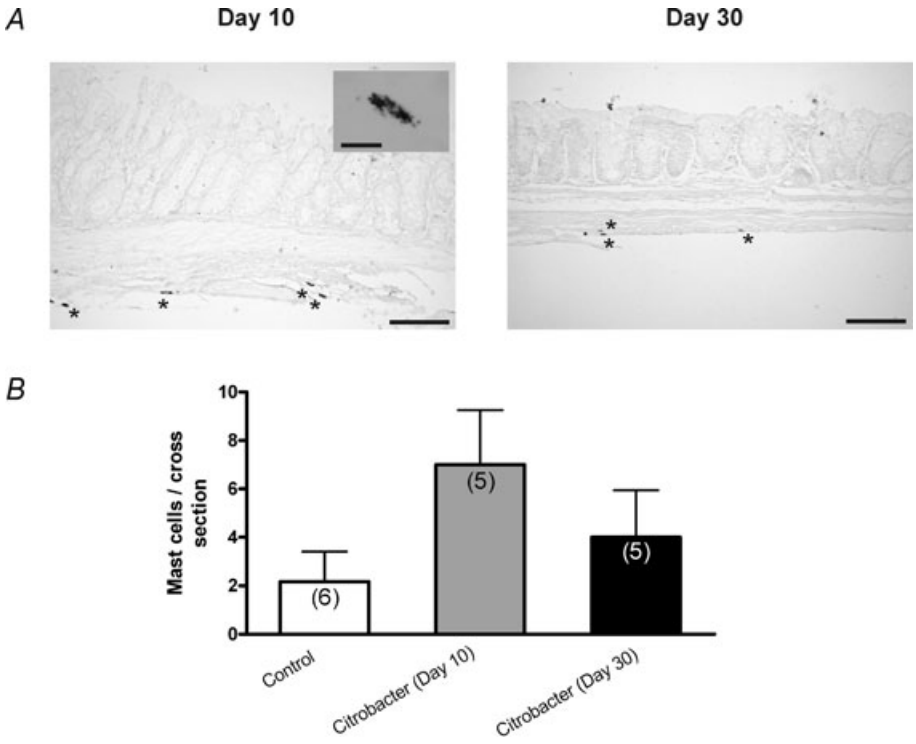

Figure 4. Assessment of mast cell numbers at day 10 and 30 following *C. rodentium* infection
A, representative photomicrographs of Toluidine Blue stained colonic tissue sections illustrating intact mast cells during active infection (day 10) and following infection resolution (day 30). Scale bar = 100 μm. Inset image shows cytoplasmic granular staining of individual mast cells (scale bar = 10 μm). *B*, summary of data ($n = 3$ sections from 5 colons) showing numbers of mast cells stained per section of colon at day 10 and day 30. Control samples from day 10 and 30 were combined. $P = 0.09$ comparing control and day 10 tissues (Mann–Whitney test).

based on their biophysical properties, as shown in Fig. 5*A*. DRG neurons from animals previously infected with *C. rodentium* exhibited a > 120% and a 36% decrease in peak current density of I_A at day 10 ($n = 15$ cells) and day 30 ($n = 14$ cells) respectively, ($P < 0.03$) compared to control neurons ($n = 11$ cells at day 10, $n = 12$ cells at day 30) (Fig. 5*B* and *C*). At day 10, neurons from *C. rodentium* infected animals also exhibited a 35% suppression of I_K peak current density ($n = 15$ cells) compared to control neurons ($n = 11$ cells), whereas, there was no significant difference in the I_K peak current density between the two groups at day 30 ($P = 0.16$).

The current–voltage relationship for the isolated currents demonstrated decreased currents in the *C. rodentium* animals near the resting membrane potential, suggesting these effects was active in the physiological range of membrane potentials (Fig. 6*A* and *B* left panel). The voltage dependencies of activation of both I_A and I_K currents in neurons from *C. rodentium* infected mice and controls were examined using a single pulse protocol (see Methods). *C. rodentium* induced colitis did not alter the voltage dependency of activation of either current. At day 10, the values for voltage of half-maximal activation, $V_{1/2}$, of I_A in *C. rodentium* and controls were -6.7 ± 1.3 mV

Figure 3. Sustained hyperexcitability of colonic DRG neurons following resolution of *C. rodentium* induced colitis
A, representative photomicrographs of H&E staining of colonic tissue sections illustrating normal histology of control tissues, increased inflammation and crypt height during active infection (day 10) and return to near normal colonic mucosal histology on resolution of infection (day 30). Scale bar = 100 μm. *B*, microscopic histological colitis scores determined by a pathologist blinded to the treatments. Mean composite scores of inflammation are shown in upper panels and mean crypt heights are shown in the lower panels for active infection on day 10 (left panels) and resolved infection on day 30 (right panels). For day 30 colons, T (all colons) and NI (non-inflamed colons only) based on microscopic inflammation scores. Values show a marked increase in inflammation at day 10 which had resolved in most colons by day 30 although some still showed subtle evidence of inflammation. ***$P < 0.0001$, **$P < 0.005$. *C*, summary data illustrating persistent hyperexcitability of nociceptive DRG neurons following resolution of infection (day 30). Neurons from *C. rodentium* treated animals fired significantly more action potentials at 2× rheobase compared to control. *$P < 0.05$. The mean rheobase was lower, but not significant in the *C. rodentium* treated neurons compared to controls.

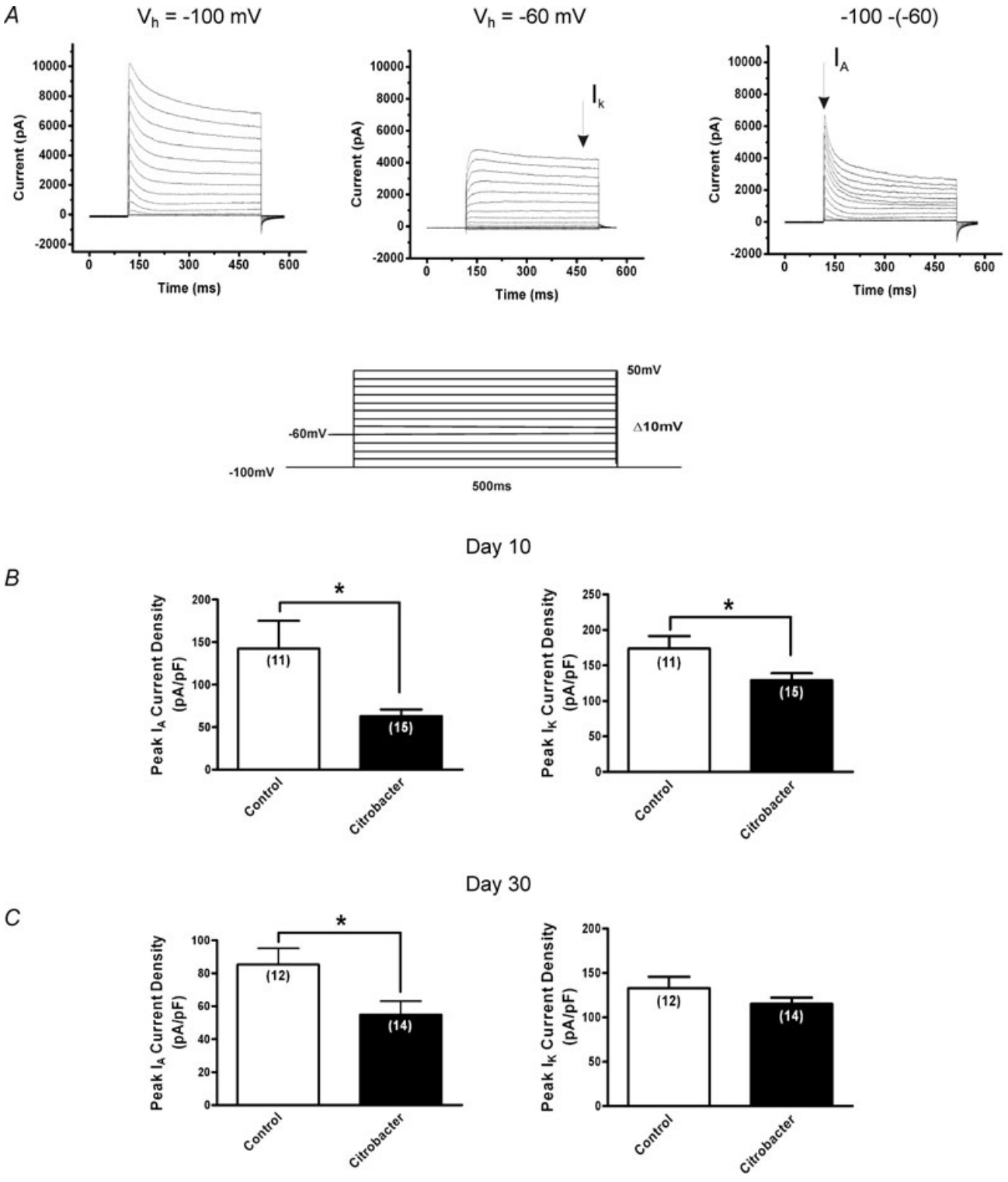

Figure 5. Effects of *C. rodentium* induced colitis on isolated voltage gated K_v currents
A, representative voltage clamp traces showing outward voltage gated K^+ current families separated biophysically by manipulating the holding potential. Currents were generated using a 10 mV voltage step protocol (illustrated in inset) from −90 mV to +50 mV. At holding potential of −100 mV (left), two currents were evident, a transient inactivating A-type current (I_A) and sustained non-inactivating I_K type currents. At a holding membrane potential of −60 mV, I_A current was significantly inactivated such that only the sustained component I_K is elicited (middle) and subtraction of the sustained from the total current yielded I_A (right). *B*, summary of peak current density for I_A and I_K respectively. Current densities were obtained by normalizing the measured amplitudes of the peak transient

and -10.7 ± 1.3 mV, respectively, with a slope factor, k, of 21.3 ± 1.4 and 20.3 ± 1.4, respectively (Fig. 6*A*). The $V_{1/2}$ values of I_K were -13.2 ± 1.0 mV and -14.0 ± 0.9 mV $P = 0.7$, with a k of 16.1 ± 1.0 and 13.2 ± 0.8, respectively (Fig. 6*A*). At day 30, $V_{1/2}$ values of I_A in *C. rodentium* and controls were -15.4 ± 1.8 mV and -14.1 ± 1.3 mV, with a k of 15.3 ± 1.7 and 14.1 ± 1.3, respectively (Fig. 6*B*).

The voltage dependency of inactivation of I_A and I_K currents was examined using a double pulse protocol (see Methods). At day 10, the half-maximal value for inactivation of I_A and I_K in *C. rodentium* neurons shifted significantly to the left compared to controls ($I_A = -76.1 \pm 0.4$ mV and -65.8 ± 0.5 mV respectively, $P = 0.0001$; $I_K = -54.6 \pm 0.4$ mV and -49.2 ± 0.1 respectively, $P = 0.001$) with k of 8.6 ± 0.4 and 9.5 ± 0.4 for I_A, 7.2 ± 0.4 and 7.5 ± 0.1 for I_K, respectively (Fig. 6*B*). At day 30 only I_A voltage dependency of inactivation (Fig. 6*B*) was examined since we did not observe any I_K current suppression at this time. The half-maximal value for inactivation of I_A in *C. rodentium* neurons was also shifted significantly to the left (as in day 10) compared to controls (-84.0 ± 0.8 mV and -74.0 ± 0.7 mV respectively; $P = 0.0001$) with k of 11.3 ± 0.7 and 10.41 ± 0.6, respectively (Fig. 6*B*). This sustained hyperpolarizing shift ($\sim$10 mV) implies that neurons from the *C. rodentium* treated animals have fewer I_A channels available at or near the resting membrane potential, leading to increased excitability and hence the increased spike frequency.

Colonic afferent fibres displayed increased mechanical discharge following *C. rodentium* infection at day 30

We used an *in vitro* model to investigate changes in visceral mechanosensitivity of colonic afferents from *C. rodentium* infected and control animals. Experiments were performed with repeated ramp distensions of the bowel, at day 10 or day 30 post-infection. We found no significant difference (unpaired t-test, $P < 0.05$) in whole nerve spontaneous activity (duration = 100 s) between control and infected animal preparations at day 10 (control 18.13 ± 4.54 spikes s^{-1}; infected 19.84 ± 3.84 spikes s^{-1}) or day 30 (control 23.05 ± 10.75 spikes s^{-1}; infected 30.01 ± 9.38 spikes s^{-1}). No differences in the afferent discharge in response to ramp distensions (60 mmHg) were observed between control ($n = 10$, one preparation per animal) and *C. rodentium* infected ($n = 10$, one preparation per animal) animals at day 10 (Fig. 7). However, the afferent discharge at day 30 post-infection ($n = 9$, one preparation per animal) was significantly augmented compared to control ($n = 10$, one preparation per animal) (Fig. 7; $P < 0.001$ two-way ANOVA).

Discussion

This study examined whether peripheral sensory mechanisms may play a role in the abdominal pain which can persist following the resolution of infectious colitis, such as found in PI-IBS. Fast Blue retrograde labelling was used to identify the DRG neurons innervating the inflamed colon and small neurons (<40 pF) were examined because numerous studies have shown they exhibit properties of nociceptors (Yoshimura & de Groat, 1999; Moore *et al.* 2002; Beyak & Vanner, 2005). We found that colitis resulting from *C. rodentium* infection for 10 days induced marked hyperexcitability of DRG neurons but had no effect on DRG neurons which did not innervate the colon. Moreover, at day 30, when histological and immune markers demonstrated the infection had resolved in the colon, colonic neurons still exhibited evidence of hyperexcitability. These findings support a role for peripheral mechanisms in the genesis of abdominal pain in conditions where symptoms persist after the inflammation has resolved, such as PI-IBS.

E. coli enteritis is one of the common causes of PI-IBS (Smith & Bayles, 2007) but the effect of bacterial induced colitis on the properties of intestinal DRG neurons has not been previously examined. We utilized *C. rodentium* because it is widely recognized as a surrogate model of human *E. coli* infection given that it has similar attachment and effacement properties and induces a self-limiting colitis (Luperchio & Schauer, 2001; Mundy *et al.* 2005). After 10 days of infection, we found that the resulting inflammation induces hyperexcitability of colonic DRG neurons, given the significant decrease in rheobase and increase in action potentials discharge at two times the rheobase. In contrast to this bacterial model of colitis, most previous studies of the effects of inflammation on visceral sensory neurons have employed models of chemical inflammation, which tends to produce a more severe inflammatory response. Despite these differences in the degree and nature of the inflammation, our electrophysiological findings were similar to those described in the models of chemical inflammation, confirming that significant changes in neuronal excitability can occur in

components of the isolated currents to the cell capacitance. At the height of inflammation (day 10), *C. rodentium* induced colitis caused significant suppression of both I_A and I_K current densities (filled bar) compared to controls (open bar). *C*, following resolution of infection (day 30), the reduction in I_A current density was sustained in neurons from *C. rodentium* infected animals (filled bar) compared to controls (open bar). There was no significant difference in I_K current density between the two groups of neurons. Data are means ± S.E.M. $^*P < 0.05$.

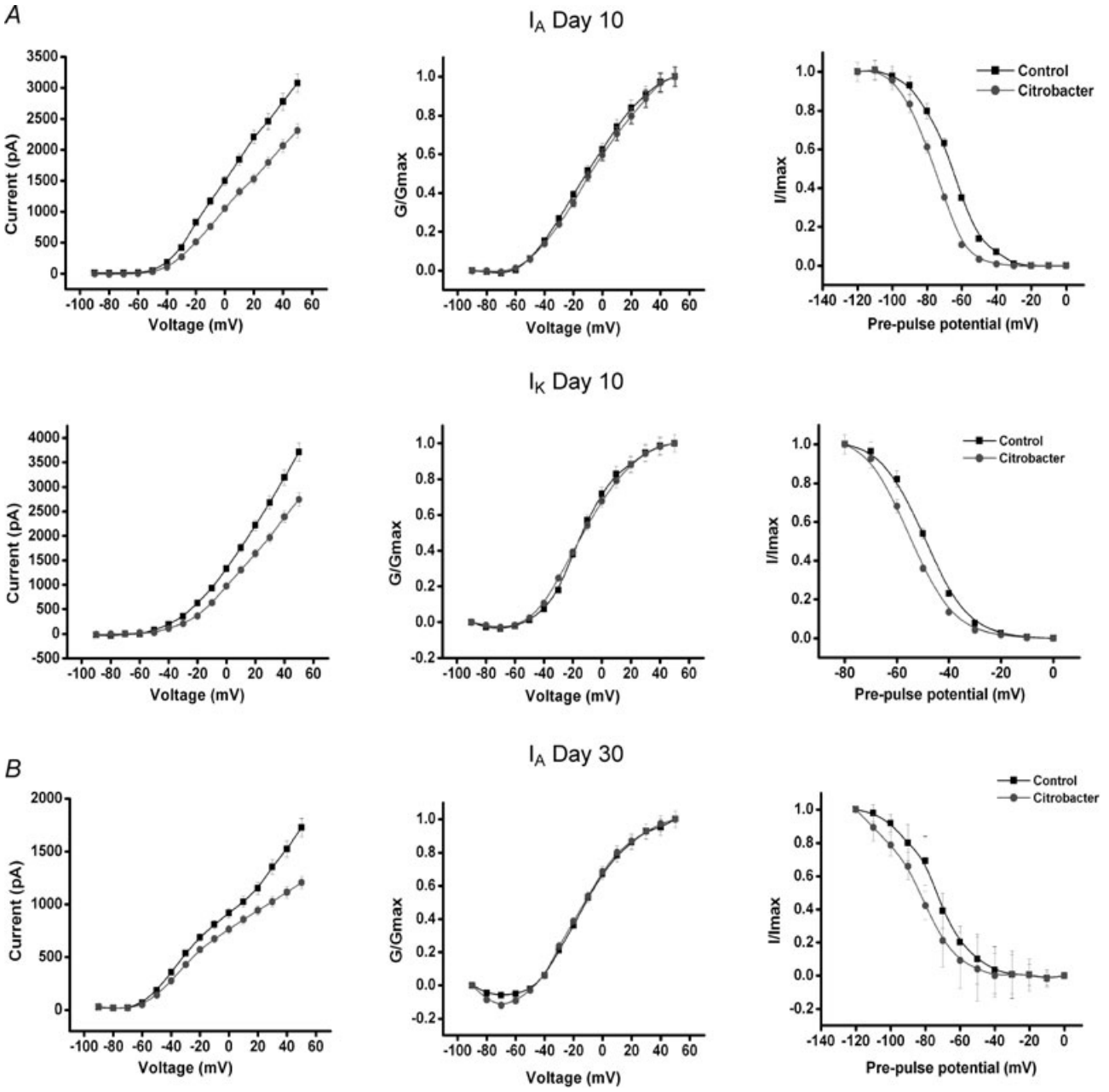

Figure 6. Effect of *C. rodentium* induced colitis on the current–voltage relationship and the steady-state activation and inactivation of I_A and I_K at the height of infection (day 10) and on resolution (day 30)
A, correlation of the current–voltage relationship for I_A (upper left panel) and I_K (middle left panel) showing significantly decreased currents by *C. rodentium* colitis near the resting membrane potential. Upper and middle central panels illustrate the steady-state activation curves for I_A and I_K from control and infected animals. Means ± S.E.M. of normalized conductance (G/G_{max}) were plotted against membrane potential. Data were fitted using Boltzmann function, and continuous lines show best fits. The upper and middle right panels show the steady-state inactivation curves for both currents in neurons from *C. rodentium* infected animals and controls. The curves were obtained by plotting the normalized test current amplitudes against conditioning pre-pulse potentials. *C. rodentium* induced colitis caused a leftward shift in the steady-state inactivation curves for both I_A (upper right panel) and I_K (middle right panel). *B*, at day 30, *C. rodentium* induced colitis also significantly decreased I_A currents near the resting membrane potential (lower left panel). The steady-state activation kinetics of I_A was not altered (lower middle panel). However, the steady-state inactivation curve for I_A currents (lower right panel) in neurons from *C. rodentium* treated animals shifted to the left (hyperpolarizing shift) when compared to controls.

the absence of severe transmural inflammation (Krauter *et al.* 2007; Lomax *et al.* 2007). One important difference was that we did not observe significant increases in input resistance, a common finding in the studies of chemical inflammation (Moore *et al.* 2002; Beyak *et al.* 2004). Although we did not explore all of the ionic mechanisms underlying this acute hyperexcitability using voltage clamp studies because this was beyond the scope of this study, this finding may suggest that the relative contribution of varying ion channels involved may differ between these models of inflammation.

If peripheral mechanisms are to play a role in the pain associated with conditions where symptoms persist after the initial inflammation has resolved, such as PI-IBS, the hyperexcitability must be sustained after the infection has resolved or be 're-primed', for example through periodic T-cell activation. At day 30, after the *C. rodentium* infection had resolved, we found that the neurons remained hyperexcitable, supporting the concept that peripheral mechanisms can contribute to the genesis of abdominal pain after infection. A recent study of a parasitic infection in the small intestine has also shown that following resolution of infection, hyperexcitability of DRG neurons persists, lending further support to the concept that peripheral mechanisms can play a role in post-infectious abdominal pain (Hillsley *et al.* 2006; Keating *et al.* 2008). This parasitic model of jejunitis is a mast cell-dependent model (Barbara *et al.*

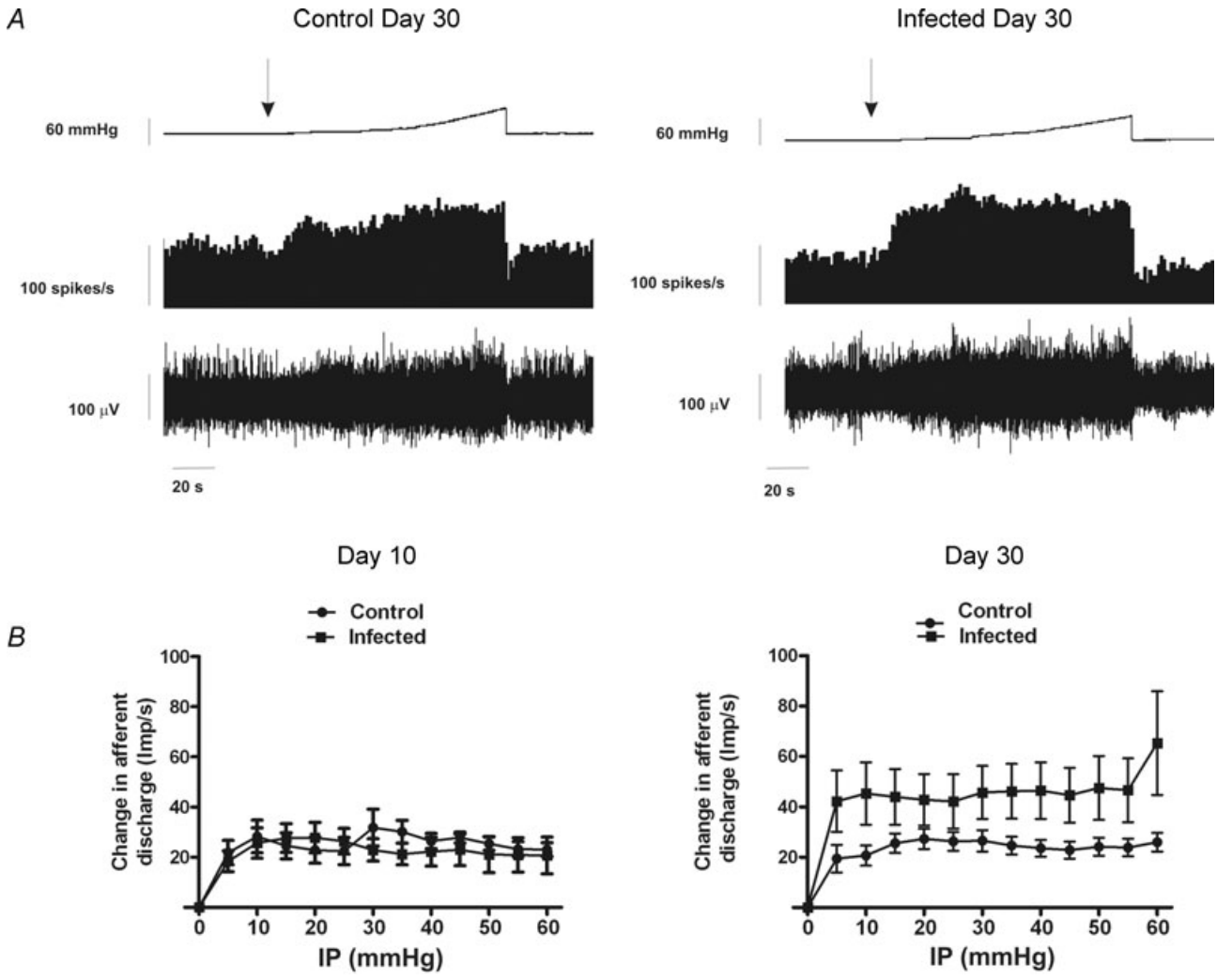

Figure 7. Assesment of visceral mechanosensitivity
A, representative trace showing pelvic nerve afferent activity (spikes s^{-1}) in response to a ramp distension in 30 days control or 30 day infected mice. Top traces, ramp distension; second trace, afferent activity rate; bottom trace, raw recording of whole nerve activity. *B*, pressure–response profiles of multi-unit activity from 10 and 30 days controls or infected animals. The pressure-response profile was significantly augmented at day 30 compared to controls ($P < 0.001$ for all measurement points, two-way ANOVA with Bonferoni's correction). Left: day 10 animals ($n = 10$); right: day 30 animals ($n = 9$). Data are means ± S.E.M. per treatment group.

2007) in contrast to the predominantly T-cell dependent mechanisms underlying *C. rodentium* and *E. coli*. Thus, it appears multiple immune pathways can induce these sustained changes in neuronal function observed in our study.

Interestingly, we did find evidence that some tissues exhibited low levels of inflammation at this late time point (i.e. day 30). However, when these were excluded from the analysis, there was still evidence of neuronal hyperexcitability (see Fig. 3). Nonetheless, clinical studies of PI-IBS have shown that activated T-cells and/or mast cells may also be contributing to visceral hyperalgesia following resolution of the colonic infection (Spiller, 2003; Hansen *et al.* 2005; Barbara *et al.* 2007). We found small numbers of intact mast cells in infected tissues at day 10. Previous studies have shown significant elevation in tissue proteases in this model during this acute infection, implying significant mast cell degranulation (Hansen *et al.* 2005). Intact mast cells were very rare at day 30 but we cannot exclude that low levels of degranulation also occurred. Changes in serotonin signalling from colonic enterochromaffin cells in patients with IBS have also been described (Mawe *et al.* 2006). Sustained hyperexcitability of DRG neurons in this setting, as found in the current study, suggests that cytokines, serotonin and/or mast cell proteases would evoke enhanced neurotransmission in nociceptive neurons compared to neurons which had not previously been exposed to an acute infection.

Multiple ionic mechanisms have been implicated in the DRG neuronal hyperexcitability observed in models of visceral inflammation (Beyak *et al.* 2004; Beyak & Vanner, 2005; Kayssi *et al.* 2007). We focused on changes in the I_A and I_K currents because our major finding at day 30 was the increase in action potential discharge numbers, which implied I_A currents may be involved. I_A has been shown to be a major current in the regulation of spiking frequency in various cell types, including neurones (Bardoni & Belluzzi, 1994) and endocrine cells (Mei *et al.* 1995). Changes in these currents have been implicated in most models of chemical inflammation (Yoshimura & de Groat, 1999; Beyak *et al.* 2004; Beyak & Vanner, 2005) but their properties have not been studied previously in models following resolution of the inflammation. We found evidence for suppression of I_A currents at day 30, which would contribute to the increased firing rate observed following resolution of the infection. It is unknown whether these persisting changes reflect altered transcription of the channel or modulation of existing channels within the membrane. It is also likely that other K^+ channels are involved, although the absence of changes in input resistance may suggest that changes in leak currents play less of a role than suggested in other models of inflammation. Given the evidence that visceral inflammation can also modulate other channels (Stewart *et al.* 2003; Beyak *et al.* 2004), further studies are needed to determine if Na^+, Ca^{2+} and/or TRP channels may also be altered by this infection (de Schepper *et al.* 2008).

We studied the physiological implications of the sustained neuronal hyperexcitability by examining the colonic afferent nerve response to ramp distentions of the colon in *C. rodentium* infected animals. These studies provide evidence for peripheral afferent hyperexcitability in the day 30 infected animals and thus support the concept that persisting changes on voltage gated ion channels in nerve terminals of DRG neurons contribute to altered sensory regulation in this post-infectious state. We were unable to perform single fibre analysis due to the high frequency response and it is possible that additional differences may exist between specific fibre types (i.e. including those at day 10 where overall differences were not seen). Recent studies suggest important differences may exist between specific fibre types and pelvic compared to splanchnic nerves in response to inflammation (Lynn *et al.* 2008; Hughes *et al.* 2009). A previous study of intestinal afferents has also shown a correlation between mechanosensitivity and neuronal hyperexcitability (Keating *et al.* 2008), although the current study is the first to identify one of the candidate ion channels (i.e. I_A currents). Not all models of inflammation, however, have provided evidence of enhanced mechanosensitivity following resolution of the inflammation (Larsson *et al.* 2006; Aerssens *et al.* 2007; Coldwell *et al.* 2007). There are no available electrophysiological correlates in these studies concerning the excitability parameters of the DRG neurons and thus it is unclear whether differences reflect the nature of the inflammation (Keating *et al.* 2008) or other contributing factors, for example 5-HT signalling or stress mediated effects that may persist following resolution of the inflammation. Indeed, there is evidence that *C. rodentium* infected animals showed increased levels of stress acutely (Lyte *et al.* 2006) and our routine handling of the infected animals to provide saline injections for hydration for the initial 5 days could also have contributed to their stress levels. Another important observation in our study concerning the relationship between neuronal excitability and mechanosensitivity was the lack of correlation between these two factors during the acute infection (i.e. neuronal hyperexcitability but no increase in mechanosensitivity). This finding mirrors a similar observation in studies of mouse small intestinal afferents (Keating *et al.* 2008) and presumably reflects an altered dynamic at the mucosal–nerve terminal interface related to the net effect of the large repertoire inflammatory mediators or other signalling pathways such as 5-HT release from enterochromaffin cells.

In summary, we found that *C. rodentium* induced colitis, a model of human *E. coli* infection, induced hyperexcitability of colonic nociceptive DRG neurons and that these changes in the intrinsic excitability of the neurons persisted after the infection had resolved,

due to suppression of I_A and possibly other channel(s). This persistent excitability could contribute to exaggerated nociceptive signalling in response to a given colonic stimulus and suggests that acute bacterial colitis could alter peripheral mechanisms of pain signalling, thereby contributing to the pain of PI-IBS. Epidemiological studies suggest that psychological factors and female sex may also be contributing factors, demonstrating the potential for interaction between central and peripheral mechanisms (Marshall *et al.* 2006). Further studies are needed in this model to evaluate these interactions.

References

Aerssens J, Hillsley K, Peeters PJ, de Hoogt R, Stanisz A, Lin JH, Van den Wyngaert I, Gohlmann HW, Grundy D, Stead RH & Coulie B (2007). Alterations in the brain-gut axis underlying visceral chemosensitivity in *Nippostrongylus brasiliensis*-infected mice. *Gastroenterology* **132**, 1375–1387.

Akopian AN, Sivilotti L & Wood JN (1996). A tetrodotoxin-resistant voltage-gated sodium channel expressed by sensory neurons. *Nature* **379**, 257–262.

Amberg GC, Baker SA, Koh SD, Hatton WJ, Murray KJ, Horowitz B & Sanders KM (2002). Characterization of the A-type potassium current in murine gastric antrum. *J Physiol* **544**, 417–428.

Azpiroz F, Bouin M, Camilleri M, Mayer EA, Poitras P, Serra J & Spiller RC (2007). Mechanisms of hypersensitivity in IBS and functional disorders. *Neurogastroenterol Motil* **19**, 62–88.

Barbara G, Wang B, Stanghellini V, de Giorgio R, Cremon C, Di Nardo G, Trevisani M, Campi B, Geppetti P, Tonini M, Bunnett NW, Grundy D & Corinaldesi R (2007). Mast cell-dependent excitation of visceral-nociceptive sensory neurons in irritable bowel syndrome. *Gastroenterology* **132**, 26–37.

Bardoni R & Belluzzi O (1994). Modifications of A-current kinetics in mammalian central neurones induced by extracellular zinc. *J Physiol* **479**, 389–400.

Barthold SW, Coleman GL, Jacoby RO, Livestone EM & Jonas AM (1978). Transmissible murine colonic hyperplasia. *Vet Pathol* **15**, 223–236.

Beyak MJ, Ramji N, Krol KM, Kawaja MD & Vanner SJ (2004). Two TTX-resistant Na^+ currents in mouse colonic dorsal root ganglia neurons and their role in colitis-induced hyperexcitability. *Am J Physiol Gastrointest Liver Physiol* **287**, G845–G855.

Beyak MJ & Vanner S (2005). Inflammation-induced hyperexcitability of nociceptive gastrointestinal DRG neurones: the role of voltage-gated ion channels. *Neurogastroenterol Motil* **17**, 175–186.

Bradley PP, Priebat DA, Christensen RD & Rothstein G (1982). Measurement of cutaneous inflammation: estimation of neutrophil content with an enzyme marker. *J Invest Dermatol* **78**, 206–209.

Coldwell JR, Phillis BD, Sutherland K, Howarth GS & Blackshaw LA (2007). Increased responsiveness of rat colonic splanchnic afferents to 5-HT after inflammation and recovery. *J Physiol* **579**, 203–213.

Connor JA & Stevens CF (1971). Voltage clamp studies of a transient outward membrane current in gastropod neural somata. *J Physiol* **213**, 21–30.

Cooper K, Gates P, Rae JL & Dewey J (1990). Electrophysiology of cultured human lens epithelial cells. *J Membr Biol* **117**, 285–298.

Cummins TR, Dib-Hajj SD, Black JA, Akopian AN, Wood JN & Waxman SG (1999). A novel persistent tetrodotoxin-resistant sodium current in SNS-null and wild-type small primary sensory neurons. *J Neurosci* **19**, RC43.

de Schepper HU, de Man JG, Ruyssers NE, Deiteren A, Van NL, Timmermans JP, Martinet W, Herman AG, Pelckmans PA & de Winter BY (2008). TRPV1 receptor signaling mediates afferent nerve sensitization during colitis-induced motility disorders in rats. *Am J Physiol Gastrointest Liver Physiol* **294**, G245–G253.

Drummond GB (2009). Reporting ethical matters in *The Journal of Physiology*: standards and advice. *J Physiol* **587**, 713–719.

Ghaem-Maghami M, Simmons CP, Daniell S, Pizza M, Lewis D, Frankel G & Dougan G (2001). Intimin-specific immune responses prevent bacterial colonization by the attaching-effacing pathogen *Citrobacter rodentium*. *Infect Immun* **69**, 5597–5605.

Hansen KK, Sherman PM, Cellars L, Andrade-Gordon P, Pan Z, Baruch A, Wallace JL, Hollenberg MD & Vergnolle N (2005). A major role for proteolytic activity and proteinase-activated receptor-2 in the pathogenesis of infectious colitis. *Proc Natl Acad Sci U S A* **102**, 8363–8368.

Hillsley K, Lin JH, Stanisz A, Grundy D, Aerssens J, Peeters PJ, Moechars D, Coulie B & Stead RH (2006). Dissecting the role of sodium currents in visceral sensory neurons in a model of chronic hyperexcitability using Nav1.8 and Nav1.9 null mice. *J Physiol* **576**, 257–267.

Hughes PA, Brierley SM, Martin CM, Brookes SJ, Linden DR & Blackshaw LA (2009). Post-inflammatory colonic afferent sensitization: different subtypes, different pathways, and different time-courses. *Gut*. (in press; doi: 10.1136/gut.2008.170811).

Kayssi A, Amadesi S, Bautista F, Bunnett NW & Vanner S (2007). Mechanisms of protease-activated receptor 2-evoked hyperexcitability of nociceptive neurons innervating the mouse colon. *J Physiol* **580**, 977–991.

Keating C, Beyak M, Foley S, Singh G, Marsden C, Spiller R & Grundy D (2008). Afferent hypersensitivity in a mouse model of post-inflammatory gut dysfunction: role of altered serotonin metabolism. *J Physiol* **586**, 4517–4530.

Kellow JE, Eckersley CM & Jones MP (1991). Enhanced perception of physiological intestinal motility in the irritable bowel syndrome. *Gastroenterology* **101**, 1621–1627.

Khan MA, Ma C, Knodler LA, Valdez Y, Rosenberger CM, Deng W, Finlay BB & Vallance BA (2006). Toll-like receptor 4 contributes to colitis development but not to host defense during *Citrobacter rodentium* infection in mice. *Infect Immun* **74**, 2522–2536.

Krauter EM, Strong DS, Brooks EM, Linden DR, Sharkey KA & Mawe GM (2007). Changes in colonic motility and the electrophysiological properties of myenteric neurons persist following recovery from trinitrobenzene sulfonic acid colitis in the guinea pig. *Neurogastroenterol Motil* **19**, 990–1000.

Larsson MH, Rapp L & Lindstrom E (2006). Effect of DSS-induced colitis on visceral sensitivity to colorectal distension in mice. *Neurogastroenterol Motil* **18**, 144–152.

Lomax AE, O'Hara JR, Hyland NP, Mawe GM & Sharkey KA (2007). Persistent alterations to enteric neural signaling in the guinea pig colon following the resolution of colitis. *Am J Physiol Gastrointest Liver Physiol* **292**, G482–G491.

Luperchio SA & Schauer DB (2001). Molecular pathogenesis of *Citrobacter rodentium* and transmissible murine colonic hyperplasia. *Microbes Infect* **3**, 333–340.

Lynn PA, Chen BN, Zagorodnyuk VP, Costa M & Brookes SJ (2008). TNBS-induced inflammation modulates the function of one class of low-threshold rectal mechanoreceptors in the guinea pig. *Am J Physiol Gastrointest Liver Physiol* **295**, G862–G871.

Lyte M, Li W, Opitz N, Gaykema RP & Goehler LE (2006). Induction of anxiety-like behavior in mice during the initial stages of infection with the agent of murine colonic hyperplasia *Citrobacter rodentium*. *Physiol Behav* **89**, 350–357.

Malykhina AP, Qin C, Greenwood-van Meerveld B, Foreman RD, Lupu F & Akbarali HI (2006). Hyperexcitability of convergent colon and bladder dorsal root ganglion neurons after colonic inflammation: mechanism for pelvic organ cross-talk. *Neurogastroenterol Motil* **18**, 936–948.

Marshall JK, Thabane M, Garg AX, Clark W, Meddings J & Collins SM (2004). Intestinal permeability in patients with irritable bowel syndrome after a waterborne outbreak of acute gastroenteritis in Walkerton, Ontario. *Aliment Pharmacol Ther* **20**, 1317–1322.

Marshall JK, Thabane M, Garg AX, Clark WF, Salvadori M & Collins SM (2006). Incidence and epidemiology of irritable bowel syndrome after a large waterborne outbreak of bacterial dysentery. *Gastroenterology* **131**, 445–450.

Mawe GM, Coates MD & Moses PL (2006). Review article: intestinal serotonin signalling in irritable bowel syndrome. *Aliment Pharmacol Ther* **23**, 1067–1076.

Mei YA, Louiset E, Vaudry H & Cazin L (1995). A-type potassium current modulated by A1 adenosine receptor in frog melanotrophs. *J Physiol* **489**, 431–442.

Moore BA, Stewart TM, Hill C & Vanner SJ (2002). TNBS ileitis evokes hyperexcitability and changes in ionic membrane properties of nociceptive DRG neurons. *Am J Physiol Gastrointest Liver Physiol* **282**, G1045–G1051.

Mundy R, MacDonald TT, Dougan G, Frankel G & Wiles S (2005). *Citrobacter rodentium* of mice and man. *Cell Microbiol* **7**, 1697–1706.

Rae J, Cooper K, Gates P & Watsky M (1991). Low access resistance perforated patch recordings using amphotericin B. *J Neurosci Methods* **37**, 15–26.

Rodriguez LA & Ruigomez A (1999). Increased risk of irritable bowel syndrome after bacterial gastroenteritis: cohort study. *BMJ* **318**, 565–566.

Rush AM, Brau ME, Elliott AA & Elliott JR (1998). Electrophysiological properties of sodium current subtypes in small cells from adult rat dorsal root ganglia. *J Physiol* **511**, 771–789.

Skinn AC, Vergnolle N, Zamuner SR, Wallace JL, Cellars L, MacNaughton WK & Sherman PM (2006). *Citrobacter rodentium* infection causes iNOS-independent intestinal epithelial dysfunction in mice. *Can J Physiol Pharmacol* **84**, 1301–1312.

Smith JL & Bayles D (2007). Postinfectious irritable bowel syndrome: a long-term consequence of bacterial gastroenteritis. *J Food Prot* **70**, 1762–1769.

Spiller RC (2003). Postinfectious irritable bowel syndrome. *Gastroenterology* **124**, 1662–1671.

Spiller RC (2007). Is IBS caused by infectious diarrhea? *Nat Clin Pract Gastroenterol Hepatol* **4**, 642–643.

Stewart T, Beyak MJ & Vanner S (2003). Ileitis modulates potassium and sodium currents in guinea pig dorsal root ganglia sensory neurons. *J Physiol* **552**, 797–807.

Tan ZY, Donnelly DF & LaMotte RH (2006). Effects of a chronic compression of the dorsal root ganglion on voltage-gated Na^+ and K^+ currents in cutaneous afferent neurons. *J Neurophysiol* **95**, 1115–1123.

Thabane M, Kottachchi DT & Marshall JK (2007). Systematic review and meta-analysis: The incidence and prognosis of post-infectious irritable bowel syndrome. *Aliment Pharmacol Ther* **26**, 535–544.

Tierney AJ & Harris-Warrick RM (1992). Physiological role of the transient potassium current in the pyloric circuit of the lobster stomatogastric ganglion. *J Neurophysiol* **67**, 599–609.

Tornblom H, Lindberg G, Nyberg B & Veress B (2002). Full-thickness biopsy of the jejunum reveals inflammation and enteric neuropathy in irritable bowel syndrome. *Gastroenterology* **123**, 1972–1979.

Tuna B, Yorukoglu K, Unlu M, Mungan MU & Kirkali Z (2006). Association of mast cells with microvessel density in renal cell carcinomas. *Eur Urol* **50**, 530–534.

Whitehead WE & Crowell MD (1991). Psychologic considerations in the irritable bowel syndrome. *Gastroenterol Clin North Am* **20**, 249–267.

Wiles S, Pickard KM, Peng K, MacDonald TT & Frankel G (2006). In vivo bioluminescence imaging of the murine pathogen *Citrobacter rodentium*. *Infect Immun* **74**, 5391–5396.

Yoshimura N & de Groat WC (1999). Increased excitability of afferent neurons innervating rat urinary bladder after chronic bladder inflammation. *J Neurosci* **19**, 4644–4653.

Author contributions

C.I. assisted in the design of the entire study, conducted and analysed the patch clamp electrophysiological recordings, assisted in the writing, and approved the final version. M.R. and N.M. conducted and analysed the *Citrobacter rodentium* microbiology in the study including assisting with the writing of the related aspects in the study and approved the final version. D.H. designed and conducted the histopathological studies, wrote the related sections, and approved the final version. M.M.-M. designed, conducted and wrote the related sections on the afferent fibre recordings and approved the final version. F.B.-C. assisted in the design of the patch clamp recordings, contributed and analysed some of the patch clamp data, and approved the

final version. S.V. was the senior author and oversaw the design, analysis, and writing of the entire study and approved the final version.

Acknowledgements

We thank Iva Kosatka and Margaret O'Reilly for their technical support and Drs Alan Lomax and Ian Spreadbury for valuable comments on the manuscript and helpful discussions. S.V. is supported by an operating grant from CIHR and a scientist award from CCFC. C.I. is supported by the GIDRU CIHR Training Grant in Digestive Sciences.